International Journal of ChemTech Research
CODEN (USA): IJCRGG, ISSN: 0974-4290, ISSN(Online):2455-9555
Vol.9, No.08 pp 453-464, 2016

Synthesis of Fe-TiO_2 Nanoparticles for Photoelectrochemical Generation of Hydrogen

Álvaro Realpe*, Diana P. Núñez, Adriana Herrera

Department of Chemical Engineering, Research Group of Modeling of Particles and Processes, University of Cartagena, Cartagena, Colombia

Abstract : In this paper, nanostructured photoanodes were made from titanium dioxide (TiO_2) nanoparticles doped with Fein order to modify its absorption range in the electromagnetic spectrum. The TiO_2 nanoparticles were obtained by a green biological route, using an extract derived from leaves of lemon grassas a reducingagent; these nanoparticles were doped by wet impregnation mechanism and supported like thin films prepared by Dr.Blading method. The morphology, structure and optical properties were evaluated by scanning electron microscope (SEM), X – ray diffraction (XRD),UV-VIS diffuse reflectance spectroscopy (UV-VIS/DRS) and photocurrent measurements. The characterization shows nanoparticles with the photoactive anatase phase of $TiO_2$with an approximate size of 56 nm. Doping of Fe^{+3} in TiO_2 resulted in a shift of absorption edge towards the visible region of solar spectrum, it was observed a decrease in the band gap energy from 3.08 to 2.66 eV with increasing the doping concentration from 0 % w/w Fe up to1.0 % Fe. The 0.5 % w/w Fe doped TiO_2 photoelectrode exhibited the highest photocurrent, 225 μA at zero external bia.
Keywords: Titanium Dioxide, Photoelectrode, Doped Nanoparticle, Band Gap, Photoelectrochemical Water Splitting.

1. Introduction

Renewable energy has gained importance due to efforts to reduce the environmental pollution. This type of energy resource has a relevant role in world's future (future world stability) due to the adverse environmental impacts of fossil based generation, besides the fact that, renewable energy resources can provide a reliable and sustainable supply of energy almost indefinitely. These sources can include solar energy, hydro energy (hydropower), biomass technology, wind power and geothermal energy [1,2,3].Currently the usage of technologies based on renewable energy has spread throughout the world to provide electricity, industrial application such as heating and drying [4].

In recent years, much attention has been paid to hydrogen, as a fuel and energy carrier [5-7];it can be used for a wide variety of applications to supplement or to substitute the hydrocarbon fuels and fossil fuels [8-16] by virtue of its high specific energy[17].Actually, the most common methods to obtained energy are based on fossil fuels (e.g., steam reforming of natural gas or other light hydrocarbons, gasification of coal and other heavy hydrocarbons), but these process are associated with high levels of CO_2 emissions[17, 18] other alternatives include electrolysis of water[5-7], direct and indirect thermochemical decomposition [19].However, water electrolysis process uses the electricity generated by fossil fuels, for that reason it is necessary to develop alternative methods that provide the electricity required of hydrogen generation by this mechanism. Renewable resources like solar and wind energyare sustainable methods for hydrogen production with high purity, simple and green process[20-23].Solar energy is regarded as one of the most promising renewable energies to support

the sustainable development of human society [24]. According to [18] the most promising way of producing hydrogen using a renewable source is through of solar energy.

Photoelectrochemical water splitting mechanism involves the splitting of water into its component gases (oxygen and hydrogen) using solar energy, in this conversion system a semiconductor photoelectrode immersed in aqueous electrolyte absorb photons and use the energy to enable a redox chemical reaction [18, 25]. Semiconducting oxides appear to be the most promising materials for photo-electrodes due to the fact that their properties may be modified over a wide range through changes in nonstoichiometry and the associated semiconducting properties[18].TiO_2 is a metal oxide semiconductor known for a wield range of applications due to its chemical stability, electronic properties, resistance to corrosion and photocorrosion in aqueous environments, non-toxicity, absorbing photochemical properties and its relatively low cost [26-28]. On account of this properties and the due to its band edges of conduction and valence matching with the redox level of the water has been subject of studies aiming at the characterization of its properties and their modification in order to use it in photoelectrochemical generation of hydrogen process [29]. Because of large band gap energy in the two main polymorphs of TiO_2(3.2 eV for anatase, 3.08 for rutile), it could only excited by UV light irradiation ($\lambda < 380$ nm), which accounts for 4% of the incoming solar energy on the Earth's surface, which leads to a very low theorical conversion efficiency [24, 28, 29]. In addition, the high recombination rate of the photogenerated electron - hole pairs ($\overline{e_{CB}}$ / h^+_{VB}) on the nanosecond time scale, results in low efficiency in utilizing photon[26-32].

A large amount of research has been focused on improving of the visible light absorption capacity in wide band gap of semiconductors through modification of its optical absorption coefficient by sensitization with small band gap organic semiconductors and/or through narrowing of its band gap via doping[33-36]. It is also important improving the morphology and electronic structure of TiO_2 for effective separation and transportation of photoexcited charge carriers[37]. Doping opens up the possibility of changing the electronic structure of TiO_2 nanoparticles, altering their chemical composition and optical properties [38], by permitting more light can be utilized to initiate the photovoltaic process [39]. Doping with metal and non-metal has been studied to change optical and electronic properties of TiO_2 that limit the efficiency in the photochemical processes, the photoactivity under visible light irradiation of metal-doped TiO_2(including transition metals) is due to a new energy level that is introduced in the band gap by the dispersion of metal particles in the TiO_2lattice, in addition, transition metal doping improvement trapping of electrons to inhibit electron– hole recombination[40]. However, the effect of the dopant depends of its abilities to trap and transfer electrons or holes [41], and its concentrations is anessential factor to determine the photoactivity of the TiO_2[42]. Transition metals such as Nb, Mn, Fe, Co, Sn, Cd, and Ni have been investigated with this purpose, between these, iron has been considered an appropriate candidate due to similar size of Fe^{3+} and Ti^{4+} ion radius, 0.64 Å and 0.68 Å respectively, therefore, Fe ions might easily be incorporated with the crystal lattice of TiO_2[28, 29, 39].Many different techniques has been reported for doping of TiO_2including sol – gel spin coating [29, 43], wet impregnation method [44], hydrothermal [45], oxidative pyrolysis [38 46].

In the present study, Fe doped TiO_2nanostructured photoanodes has been elaborated for its evaluation in a photoelectrochemical water splitting process. TiO_2 nanoparticles were synthetized by "green synthesis" mechanism, and the doping was made by wet impregnation method with different concentrations of Fe. The effect of iron doping on photoelectrode behavior was studied for band gap determination of doped and undoped photoelectrodes.

2. Experimental Procedure

2.1 Materials and methods

TiO_2 nanoparticles were synthetized by green synthesis method, using extract derived from leaves of lemon grass, the process was divided in two stages: natural extract elaboration and synthesis of TiO_2 nanoparticles. Titanium tetraisopropoxide (TTIP, 95% pure) manufactured byAlfaAesar was used as a TiO_2 precursorwhile ferric chloride hexahidrate ($FeCl_3$ $6H_2O$) as the precursor of Fe. Ethanol (CH_3CH_2OH) was used to wash of nanoparticles. TiO_2 thin films were supported over stainless steel sheet (5×5 cm^2 area and 0.3 mm thick, SS 304), prior to its use, stainless steel sheet was rigorously cleaned using soapy water, acetone, isopropanol and distilled water, and then dried in ambient air. After that, it was immersed in 0.5 M acid sulfuric

solution followed by rising with distilled water[47]Acronal 295 D (acronal – water 50% v/v) as adhesive to TiO_2 impregnation,Sulfuric acid (95-97%) was used to obtain the electrolyte solution (0.1 M).

2.2 Preparation of extract derived from leaves of lemon grass

Lemon grass (*Cimbopogon cytratus)* extract was used as a reducing agent. The fresh leaves were washed with distilled water to remove the dust or any other dirt of the environment and dried at 40°C in a furnace, after that, the leaves were cut into fine pieces and grinded. Aqueous extract of lemon grass was prepared by immersion of 100 g of lemon grass in 500 ml of distilled water at 100°C and was left at rest. This extract was filtered through filter paper several times and concentrated by evaporation, heating it at 80°C until 100 ml of extract.

2.3 Synthesis of titanium dioxide nanoparticles

For synthesis of TiO_2 nanoparticles, 85 ml aqueous solution of 5 mM of titanium isopropoxide was stirred during 12 h, 15 ml of the aqueous extract of lemon grass was added in 5 mM solution with continuous stirring at 175 rpm and room temperature for 24 h [48]. After the reaction of lemon grass extract with TTIP, the solution was centrifuged and nanoparticles were collected and dispersed in ethanol and then in distilled water, the centrifugation process was repeated to wash out impurities. Finally, titanium dioxide nanoparticles were dried in an oven at 100°C and then calcined in a muffle furnace for 3 h, starting at 330°C and ending at 550°C, this heat treatment also allows the removal of organic matter without reacting [49].

2.4 Metal doping semiconductor - Preparation of Fe doped TiO_2 nanoparticles

TiO_2 nanoparticles were doped using wet impregnation method [36]. An amount of TiO_2 was added in distilled water, the TiO_2 slurry was stirred for 30 min (to break up the loosely attached aggregates), after, an aqueous solution of iron (III) chloride (precursor of Fe^{+3}) with the required amount of precursor required for doping was added to TiO_2 suspension. It was subject to continuous stirring at room ambient for 48 h, and subsequently driedat 80°C, the solid was then crushed and calcined in a muffle furnace at 400°C for 2 h[50]. The Fe concentration were of 0.5, 0.7 and 1.0 % w/w versus TiO_2.

2.5 Elaboration of nanostructured photoelectrodes

To make the photoelectrodes, TiO_2 thin films were supported over stainless steel sheets. The suspension was prepared by adding TiO_2 nanoparticles to acronal solution (40% w/v TiO_2 – acronal), the suspension was magnetically stirred for 30 min, and an ultrasonic bath was using to improve the dispersion state of nanoparticles in solution [51], it was used acronal in the suspension to ensure the films adhesion over the substrate. The suspension (paste) was applied onto the stainless steel sheet by a technique reported by [52-55],after deposition, the film was allowed to dry in air. The deposited process was repeated two more times to obtain a multilayer film (three layers), after that, films were subject to thermal treatment of sintering at 400°C for 30 min [49, 55-57], sintering allows of evaporating the solvent, to improve the nanoparticles connectivity, mechanical strength and the electrical conductivity of the photoelectrode [57].

2.6 Characterization

2.6.1 X – ray Diffraction analysis (XRD)

X-ray diffraction analysis was performed to identify crystal phase of titanium dioxide nanoparticles using a Bruker Model D8 ADVANCE Diffractometer.

2.6.2 Scanning electron microscopy (SEM)

SEM analysis was performed on a Quanta 650 FEG Scanning Electron Microscope, through this analysis was identified the particle size and morphology of nanoparticles synthesized.

2.6.3 V-VIS diffusion reflectance spectroscopy (UV-VIS/DRS)

The UV-Visible diffuse Reflectancia spectra was measures in the wavelength from 200 to 800 nm using a Thermo Scientific EVOLUTION 600 spectrophotometer UV/VIS. The spectra were obtained in reflectance percentage (%R).

2.6.4 Photoelectrochemical characterization

Spectral photocurrent was measured in a configuration of two electrodes[58] into a photo electrochemical cell with a TiO_2 photoelectrode as a working electrode and a stainless steel counter electrode introduced in an aqueous 0.1 M sulfuric electrolyte solution. The measurement of the electrical parameter was carried out using a multimeter connected to the system through an external circuit, electrical contact was made with a copper wire. The photoanode was radiated with a lamp visible light. The distance between the working and the counter electrode was 15 cm. The separated of photogenerated charges was evaluated by photocurrent response under irradiation, undoped and Fe doped TiO_2 photoelectrodes were used.

3. Results and Discussion

3.1X – ray Diffraction analysis (XRD)

TiO_2 nanoparticles formation through extract derived from leaves of lemon grass was confirmed by X-ray diffraction analysis. Figure 1 displays the XRD pattern of synthesized TiO_2 nanoparticles. This figure shows well-defined peaks,indicating the crystalline nature of the phases present in the sample [59].These peaks can be denoted at 2θ value of 25.3°, 37.99°, 48.0°, 54.5°, 62.9°, which are characteristic ofthe Anatase phase of TiO_2[60]. In this DRX pattern are not present the diffraction peaks belonging to the other polymorphs of TiO_2, rutile and brookita [60]. An important factor towardthis result is the calcination temperature of the nanoparticles, it has been reported[61], that normally anatase-rutile phase transformation takes place in the temperature range from 600 to 700°C, in accordance with [62], the temperature range for anatase–rutile transformation shifted to higher temperature with the increase of the synthesized pH value. The transformation can be also affected by factors such as preparation conditions, precursors, impurities, oxygen vacancies and the particle size of the anatase phase obtained [61].

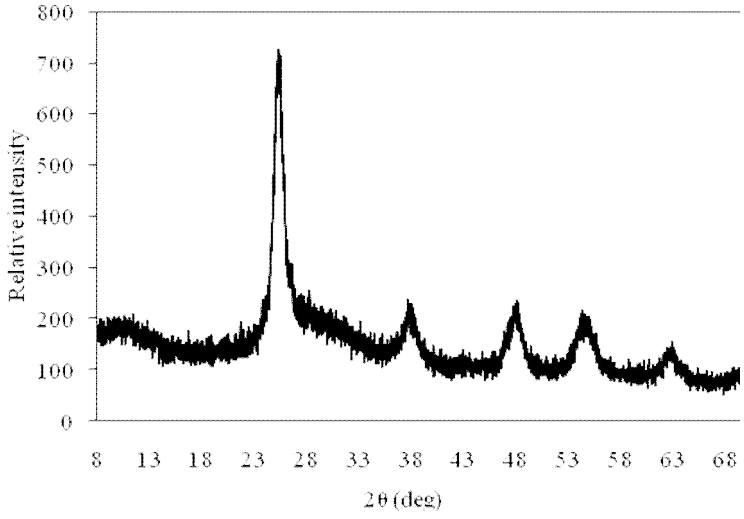

Figure 1. XRD pattern of TiO_2 nanoparticles synthesized from aqueous leaf extract of *lemon grass*

The synthesis of TiO_2nanoparticles has been investigated using different plant species, by using *Aloe vera* extract [63], *Eclipta prostrata* leaf[40], *Jatropha curcas* [64].These investigations report that biosynthesis of TiO_2 nanoparticles through extract from plantsoccur due to phytochemicals as terpenes, ketones, aldehydes and flavonoids, which are the main responsible of the reactions because they may act as reducing agents of alkoxide, which gives rise to the formation of the nanoparticles of TiO_2.

3.2Scanning electron microscopy (SEM)

Figure 2 shows the scanning electron microscope (SEM) of pure TiO_2 nanoparticles synthesized by green synthesis method. According to the micrograph, the morphology of the TiO_2 nanoparticles is approximately spherical, the nanoparticles are agglomerated together to form lot of nanoclusters.

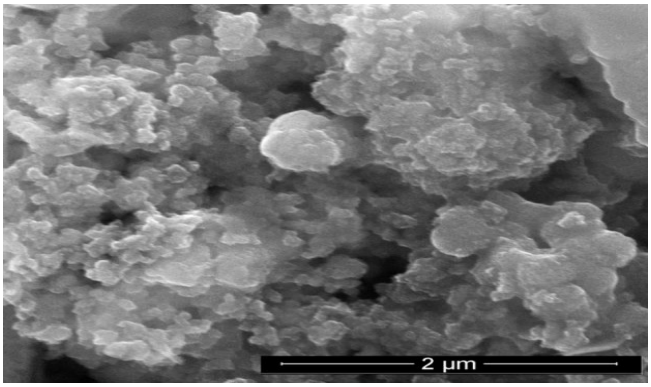

Figure 2.SEM micrograph of TiO_2 nanoparticles

The nanoparticles size distribution analysis was carried out using ImageJ program, the particles are distributed in the size 56±16 nm ranges. Figure3 shows the histogram corresponding to that distribution.

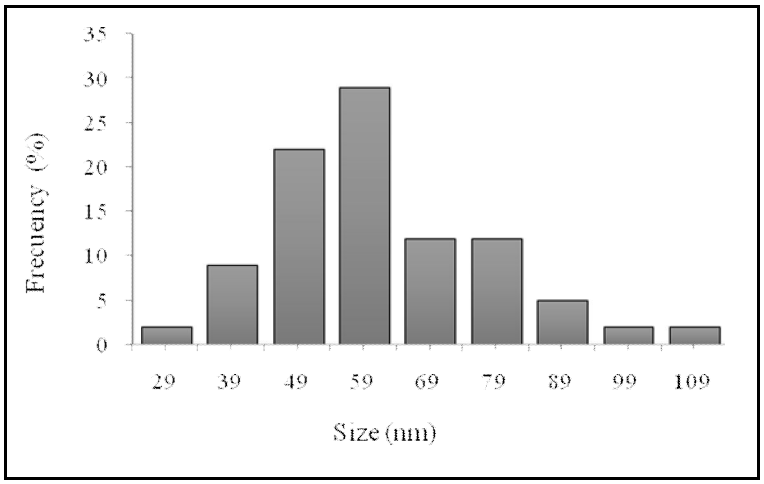

Figure 3.TiO_2 nanoparticles histogram

3.3UV-VIS diffuse reflectance spectroscopy (UV-VIS/DRS)

Figure 4 shows the optical reflectance diffuse properties of undoped TiO_2 and doped TiO_2 with Fe, and to form the thin films deposited on stainless steel sheets for studying with ultraviolet-visible (UV-vis) in the wavelength range of 200 - 800 nm. It reveals that incorporation of iron ions leads to shift of optical response toward visible part of the spectra.

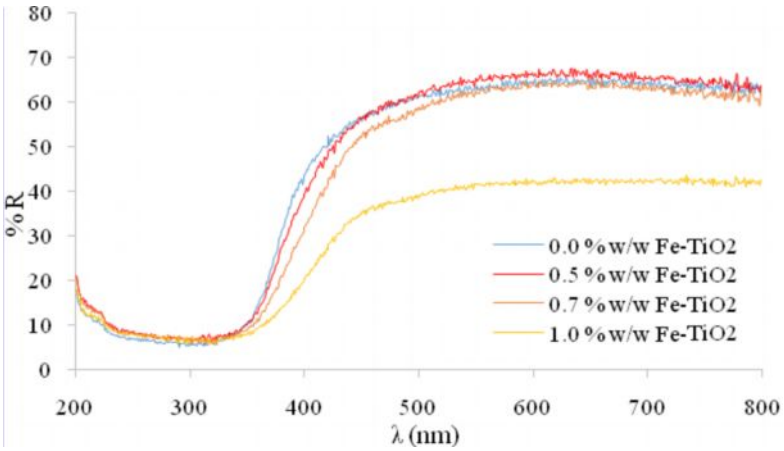

Figure 4.Diffuse reflectance spectra of Fe doped TiO_2 films supported

The optical energy band gap of undoped and Fe doped TiO_2 were determined using theTauc plotmethod $\alpha h\upsilon = A(h\upsilon - E_g)^n$, where α is the absorption coefficient, A is constant, $h\upsilon$ is the photon energy, E_g is the optical band gap energy and n denote the nature of the electronictransition interband [65-67], the absorption coefficient $(\alpha$)was determined by applying Kubelka – Munk function [68-69], the equation for this method is represented by $F(R) = \frac{(1-R)^2}{2R}$, where R is the reflectance and $F(R)$ is the reflectance function which is proportionally to absorption coefficient $(\alpha$). For anindirect optical transition in anatase TiO_2[69], was plotted $(\alpha h\upsilon)^{1/2}$ as a function of the$h\upsilon$ Figure 5, the linear part of those graphs was extrapolated to$(\alpha h\upsilon)^{1/2} = 0$ (the energy axis), allowing to determine band gap$[(E]_g)$.

As indicating in Table 1, the band gap energy for undoped film is higher than band gap energy of Fe doped TiO_2 films, the value of this energy gap reduces with increasing of Fe concentration, these results are in agreement with other investigations [29], [70] in which have reported that the band gap energy was reduced as the Fe concentration increases. The band gap values decreased from 3.09 eV to 2.66 eV with an increase in the Fe content from 0 to 1.0 % w/w. Some authors have found that the optical energy band gap does not change from a determined concentration of doping, Tae-hyun Lee et al reported a decrease of E_g value from 3.0 to 2.2 eV at 0 % and 2 % of Fe, but with concentration increase at 5, 10 and 20 % band gap energy of films increased to 2.8 and 2.9 eV, without shows a change for the latest (10 and 20 %) [66].

Table 1. Band gap energy and photocurrent of Fe doped TiO_2 films at different doping concentration

Sample	Band gap energy (Ev)	λ (nm)	Photocurrent (μA)
Undoped TiO_2	3.09	401.94	-
0.5 % w/w Fe- TiO_2	3.02	411.258	87.4
0.7 % w/w Fe- TiO_2	2.89	429.757	133.12
1.0 % w/w Fe- TiO_2	2.66	466.91	112.62

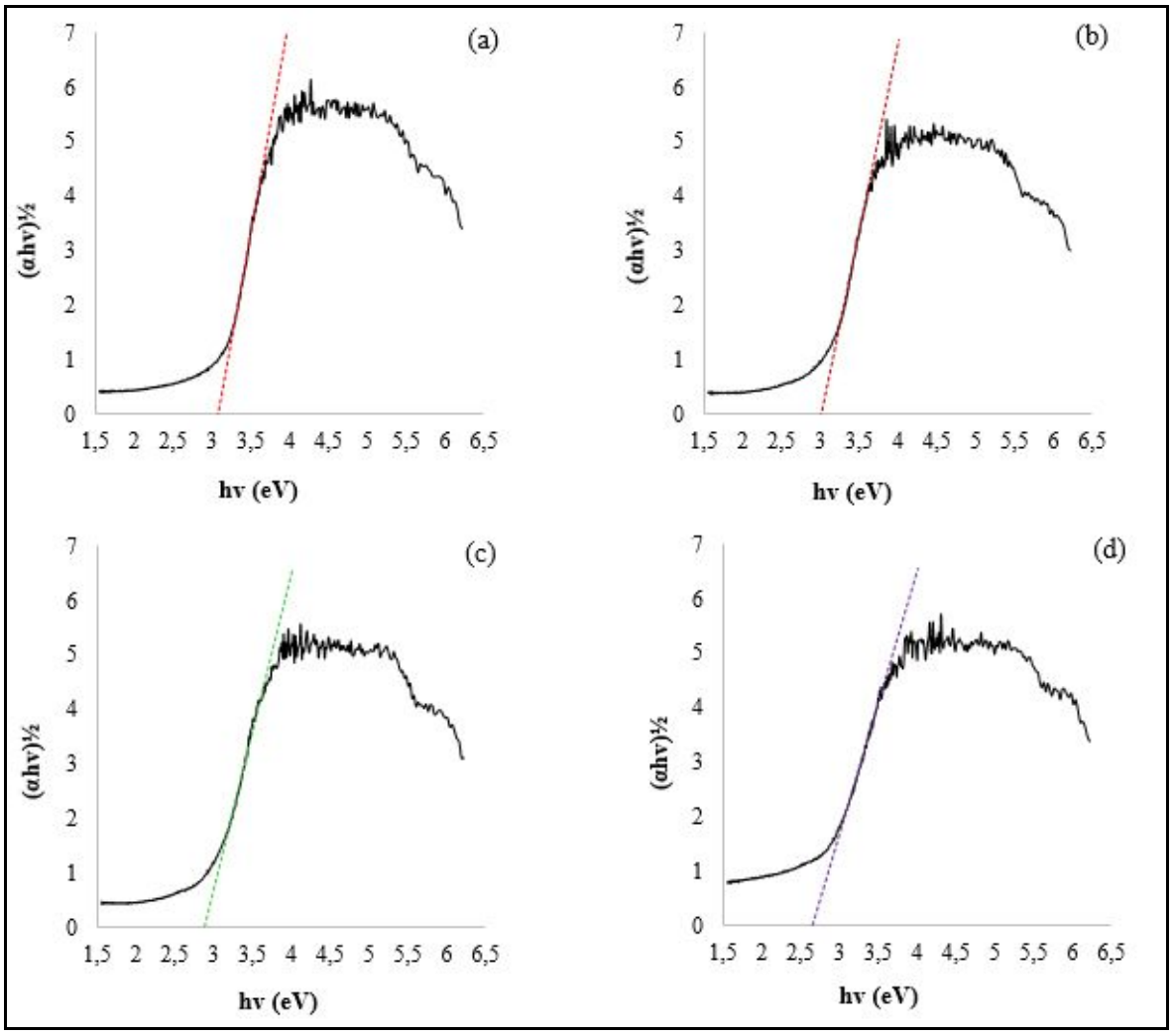

Figure 5. Relation$(\alpha hv)^{1/2}$ and the photon energy of Fe – doped TiO_2 nanoparticles. (a) 0 % w/w Fe, (b) 0.5 % w/w Fe, (c) 0.7 % w/w Fe, (d) 1.0 % w/w Fe.

In according to[60] by doping is achieved a modification in electronic structure of the semiconductor, through it, additional electronic states can be provide within the band gap of the TiO_2. Therefore, the shift of absorption edge toward visible region is due to the electron excitation and transfer from these levels (dopant ions) to the conduction band of TiO_2 requires photons with low energy than an electron excitation and transfer from the valence to conduction band [61, 71-72].In this case, the visible region is induced by a sub-band gap transition between the 3d electrons of Fe and the conduction band of TiO_2 [73-74].

3.4 Photoelectrochemical characterization

Figure 6displays the photocurrent generated by the photoelectrodes under dark and illuminated conditions (visible light), without applying an external voltage for the measurements. As a result of visible light excitation in doped photoelectrodes, photocurrent trough the cell between photoanode and cathode, therefore, the addition of Fe did provide visible light absorptionin TiO_2.The graphics show an increase of the photocurrent after the photonic source was turned on. The photocurrent generated when visible light was used on Fe doped TiO_2 photoelectrodes allowed the generation of gases in the photoelectrochemical cell. Undoped TiO_2 photoelectrode does not shows response under visible light irradiation.

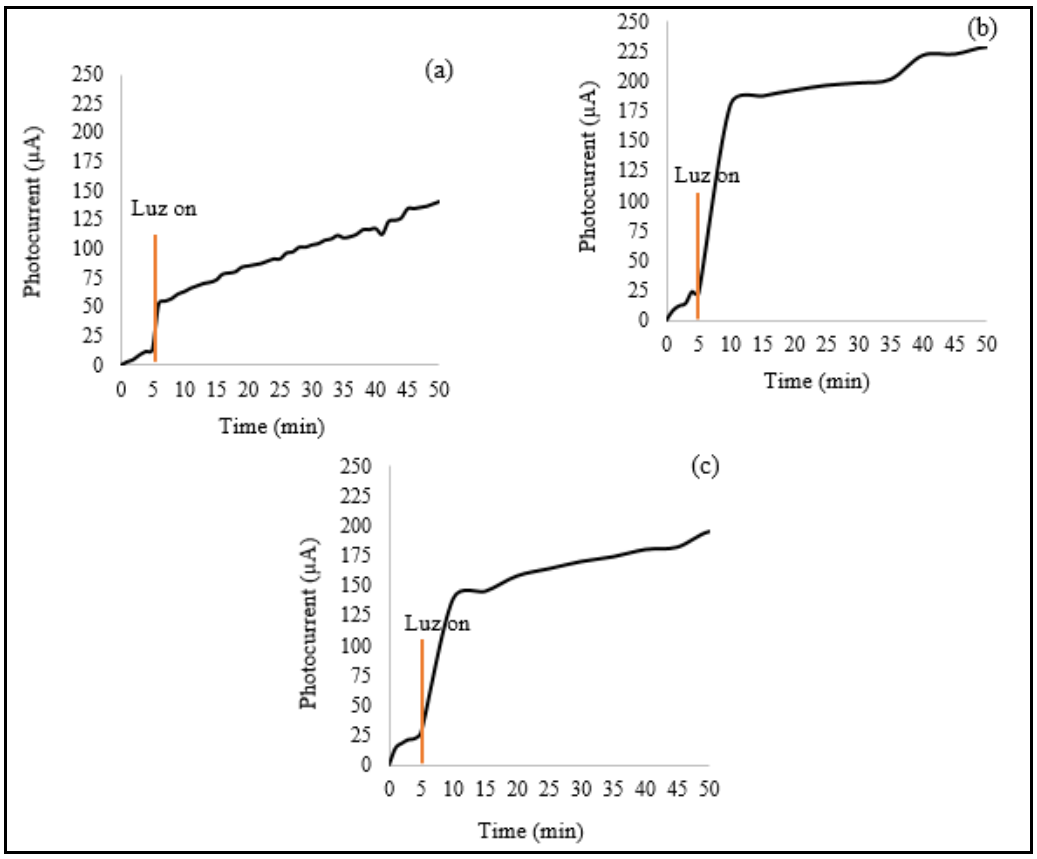

Figure 6.Photocurrent as a function of time without bias voltages under illumination by visible light: (a) 0.5 % w/w Fe-TiO_2 - (b) 0.7 % w/w Fe-TiO_2 - (c) 1.0 % w/w Fe-TiO_2

The 0.7 % w/w Fe doped TiO_2 exhibited the highest photocurrent, which was 133.12 µA at zero external bias, above and below this doping photocurrent was lower. It was 87.04 µA for 0.5 % w/w and 112.62 µA for 1.0 % w/w. According to [29]this performance may be attributed to traps created within the band gap, which act as trapping center for photogenerated electron – hole pair, hence it may prolong the charges lifetime, increasing the recombination time, however, the photocurrent with 1.0 %w/w Fe decrease because at high doping concentration the recombination of this photogenerated charges is easier.[66] reported in their investigation that the photocurrent decreased when doping concentration increased due to agglomeration, because it is more difficult for photoexcited minority carriers to escape to the electrolyte. Therefore, there is an optimal dopant concentration that allowed the photoactivity reaches maximum values.

This values of photocurrent can be comparable to [75] where under similar conditions (without external bias) were obtained lower photocurrent values in TiO_2 photoelectrode, in [21]and [22] were obtained higher photocurrent values. From graphics can be observed that happened fluctuations in photocurrent behavior over time, one of the reasons for declines in the values of photocurrent occur is due to accumulation of bubbles (gas) on the photoelectrodes surface, which leads to a decrease in its effective area [75].

4. Conclusions

In this investigation, TiO_2 nanoparticles were synthetized to elaborate photoelectrodes. The used method for synthesis allowed to obtain nanoparticles with a ban gap lower than some commercial semiconductors with a small particle size, hence it could be a viable alternative since it is also simple, low cost and environmental benignant. The incorporation of Fe into the lattice of pure TiO_2 by wet impregnate reduced its bang gap from 3.09 eV to 2.66 eV, shifting the absorption edge of TiO_2 toward a region of lower energy, the largest reduction was obtained with a 1.0 % w/w Fe concentration. With all Fe-TiO_2 photoelectrodes photocurrent was generated through visible light radiation without bias external, the better behavior photocurrent was observed in 0.7 % w/w Fe – TiO_2 photoelectrode reaching 133.12 µA.

Acknowledgements

The authors of this investigation are grateful to Administrative Department of Science, Technology and Innovation (COLCIENCIAS, Colombia) and to the University of Cartagena for finance and provide the space for perform this project through the program of researcher young and innovator 2015.

References

1. Realpe A., Brenda Chamorro, Modeling and Assessment of Wind Energy Potential in the Cartagena City, International Journal of ChemTech Research, Vol.9, No.5, 2016, pp 614-623
2. Realpe A., J. Diazgranados, M. Acevedo, Electricity generation and wind potential assessment in regions of Colombia, DYNA, Vol. 79, núm. 171, 2012.
3. Hori K, Matsui T, Hasuike T, Fukui K, Machimura T. Development and application of the renewable energy regional optimization utility tool for environmental sustainability: REROUTE. Renewable Energy. 2016, August; 93: 548-561.
4. Realpe Alvaro, Randy Reina, Andrea Figueroa, Adriana Herrera, María Acevedo, Modeling of a solar collector of parabolic dish and a plate heat exchanger to improve the industrial drying process of calcium propionate, accepted for publication in International Journal of ChemTech Research, Vol.9, No.7, 2016.
5. Realpe A, Salamanca A, Acevedo M. Effect of electrolyte type on the hydrogen production using a plate electrolyzer. International Journal of Applied Engineering Research. 2015; 10(9): 23871 – 23880.
6. Realpe A, Salamanca A. Effect of spacing between electrodes on the hydrogen generation. International Journal of Applied Engineering Research. 2015; 10(14): 34262 – 34264.
7. Realpe A, Orozco A, Acevedo M. Wind power for hydrogen production using a spiral electrolyzer. International Journal of Applied Engineering Research. 2015; 10(4): 9175 – 9183
8. Arokia Pushpa Agal, N.T. Mary Rosana, D. Joshua Amarnath, Assessment of Solar Energy Opportunity in a Bicycle Manufacturing Plant, International Journal of ChemTech Research, Vol.8, No.4, 2015, pp 1783-1790
9. Dhanuskodi. S, R. Sukumaran, Vincent .H. Wilson, Investigation of Solar Biomass Hybrid System For Drying Cashew, International Journal of ChemTech Research, Vol.5, No.2, 2013, pp 1076-1082
10. Realpe A, Mendez N, and Acevedo M, Proton Exchange Membrane from the Blend of Copolymers of Vinyl Acetate-Acrylic Ester and Styrene-Acrylic Ester for Power Generation Using Fuel Cell, International Journal of Engineering and Technology, 6(5), 2014, pp 2435-2440.
11. Srimanta Ray, Ajoy Chakraborty and Debika Debnath, Development of a Cost-Optimized Hybrid Off-Grid Power System For a Model Site in North-Eastern India Involving Photovoltaic Arrays, Diesel Generators and Battery Storage, International Journal of ChemTech Research, Vol.5, No.2, 2013, pp 771-779
12. Balamurugan. R, Srinivasan. K, Balasubramanian. K, Anand. M, and Ravisankar. G, Future Constructions Using Renewable Energy, International Journal of ChemTech Research, Vol.5, No.3, 2013, pp 1186-1194.
13. Farooq Ahmad Najar, G A Harmain, Blade Design and Performance Analysis of Wind Turbine, International Journal of ChemTech Research, Vol.5, No.2, 2013, pp 1054-1061.
14. Manoj Verma, Pankaj Sahu, Siraj Ahmed, J.L.Bhagoria, Analysis of Wind Characteristics in and Around Open Cast Uranium Mine, International Journal of ChemTech Research, Vol.5, No.2, 2013, pp 601-609.
15. Vipin Kumar Singh, Tiju Thomas, Vilas Warudkar, Structural Design of a Wind Turbine Blade: A Review, International Journal of ChemTech Research, Vol.5, No.5, 2013, pp 2443-2448.
16. Realpe A, Karoll Romero, Anny Santodomingo, Synthesis of a Proton Exchange Membrane from Vinyl Acetate - Acrylic Ester Copolymer for Fuel Cells, International Journal of ChemTech Research, Vol.8, No.3, 2015, pp 1319-1326
17. Midilli A, Ay M, Dincer I, Rosen MA. On hydrogen and hydrogen energy strategies: I: current status and needs. Renewable and Sustainable Energy Reviews. 2005, June, 9(3): 255 – 271.
18. Nowotny J, Sorrell CC, Sheppard LR, Back T. Solar – hydrogen: Environmental safe fuel for the future. International Journal of Hydrogen Energy. 2005, April; 30(5): 521 – 544.
19. Steinfeld A. Solar thermochemical production of hydrogen – a review. Solar Energy. 2005, May; 78(5): 603 – 615.

20. Abanades S, Charvin P, Flamant G, Neveu P. Screening of water – splitting thermochemical cycles potentially attractive for hydrogen production by concentrated solar energy. Energy. 2006, November; 31(14). 2805 – 2822.
21. Realpe A, Núñez D, Carbal I, Acevedo M, De Ávila G. Preparation and Characterization of Titanium Dioxide Photoelectrodes for Generation of Hydrogen by Photoelectrochemical Water Splitting. International Journal of Engineering and Technology. 2015; 7(2): 753-759.
22. Realpe A, Núñez D, Carbal I, Acevedo M, De Ávila G. Sensitization of TiO2 Photoelectrodes Using Copper Phthalocyanine for Hydrogen Production. International Journal of Engineering and Technology. 2015; 7(4): 1189-1193.
23. Experimental wind to hydrogen system up and running [Internet] 2007 January 8. Available from: http://www.physorg.com/news87494328.html〉.
24. Shi Z, Wen X, Guan Z, Cao D, Luo W, & Zou Z. Recent progress in photoelectrochemical water splitting for solar hydrogen production. Annals of Physics. 2015, July; 358: 236-247.
25. Turner J, Sverdrup G, Mann MK, Maness PC, Kroposki B, Ghirardi M, Evans RJ, Blake D. Renewable Hydrogen production. International journal of Energy Research. 2008; 32(5): 379 – 407.
26. Fujishima A, Rao TN, Tryk DA. Titanium dioxide photocatalysis. Journal of Photochemistry and Photobiology C: Photochemistry Reviews. 2000, June; 1(1): 1-21.
27. Nowotny J, Bak T, Nowotny MK, Sheppard LS. Titanium dioxide for solar-hydrogen I. Functional properties. International Journal of Hydrogen Energy. 2007, September; 32 (14): 2609-2629.
28. Fan X, Fan J, Hu X, Liu E, Kang L, Tang C. Preparation and characterization of Ag deposited and Fe doped TiO_2 nanotube arrays for photocatalytic hydrogen production by water splitting. Ceramics International. 2014, December; 40 (10): 15907-15917.
29. Singh A P, Kumari S, Shrivastav R, Dass S, Satsangi V. Iron doped nanostructured TiO_2 for photoelectrochemical generation of hydrogen. International Journal of Hydrogen Energy. 2008, October; 33 (20): 5363-5368.
30. Ozawa K, Emori M, Yamamoto S, Hobara R, Fujikawa K, Sakama H, Matsu I. Electron - Hole Recombination Time at TiO_2 Single-Crystal Surfaces: Influence of Surface Band Bending. J. Phys. Chem. 2014, May; 5(11): 1953-1957.
31. Cowan AJ, Tang J, Leng W, Durrant JR, Klug DR. Water Splitting by Nanocrystalline TiO_2 in a Complete Photoelectrochemical Cell Exhibits Efficiencies Limited by Charge Recombination. J. Phys. Chem. 2010, Feb.; 114 (9): pp. 4208-4214.
32. Naeem K, Ouyang F. Preparation of Fe3+ doped TiO_2 nanoparticles and its photocatalytic activity under UV light. Physic B. 2010, January; 405 (1):221-226. Preparation of Fe3+ doped TiO_2 nanoparticles and its photocatalytic activity under UV light
33. Park JH, Kim S, Bard AJ. Novel carbon-doped TiO_2 nanotube arrays with high aspect ratios for efficient solar water splitting. Nano Letters. 2006; 6(1): 24 – 28.
34. Hensel J, Wang G, Li Y, Zhang JZ. Synergistic effect of CdSe quantum dot sensitization and nitrogen doping of TiO_2 nanostructures for photoelectrochemical solar hydrogen generation. Nano Letters. 2010; 10(2):478-483.
35. Tan M, Wang H, Sun D, Peng W, Tao W. Visible light driven nanocrystal anatase TiO_2 doped by Ce from sol-gel method and its photoelectrochemical water splitting properties. International Journal of Hydrogen Energy. 2014, August; 39(25): 13448 – 13453.
36. Vigil E, Gonzáles B, Zumeta I, Domingo C, Doménech X, Ayllón JA. Preparation of photoelectrodes with spectral response in the visible without applied bias based on photochemically deposited copper oxide inside a porous titanium dioxide film. Thin solid films. 2005, October; 489(1-2): 50 – 55.
37. Wang G, Wang H, Ling Y, Fitzmorris R C, Wang C, Zhang J Z, & Li Y. Hydrogen-Treated TiO2 Nanowire Arrays for Photoelectrochemical Water Splitting. Nano Letters. 2011, June; 11 (7): 3026-3033.
38. Nasralla N, Yeganeh M, Astuti Y, Piticharoenphun S, Shahtahmasebi N, Kompany A, Karimipour M, Mendis BG, Poolton NRJ, Siller L. Structural and spectroscopic study of Fe – doped TiO2 nanoparticles prepared by sol-gel method. Scientia Iranica. 2013, June; 20(3): 1018 – 1022.
39. Zhang Y, Shen Y, Gu F, Wu M, Xie Y, Zhang J. Influence of Fe ions in characteristics and optical properties of mesoporous titanium oxide thin films. Applied Surface Science. 2009, October; 256(1): 85 – 89.
40. Zaleska, A. Doped-TiO_2: A Review. Recent Patents on Engineering. 2008, Oct.; 2 (3): 157-164.

41. Ni M, Leung M, Leung D, Sumathy K. A review and recent developments in photocatalytic water-splitting using TiO2 for hydrogen production. Renewable and Sustainable Energy Reviews. 2007, April; 11 (3): 401-425.
42. Elghniji K, Atyaoui A, Livraghi S, Bousselmi L, Giamello E, Ksibi M. Synthesis and characterization of Fe3+ doped TiO_2 nanoparticles and films and their performance for photocurrent response under UV illumination. Journal of Alloys and Compounds. 2012, November; 541: 421-427.
43. Ly NT, Dao TH, Hoang To LH, Vu DL, Hong LV. Hydrogen generation by photoelectrochemical effect of the Cu-doped TiO_2 photoanode. Advances in Natural Sciences: Nanoscience and Nanotechnology. 2014, August; 5(3).
44. Nahar MS, Hasegawa K, Kagaya S, Kuroda S. Comparative assessment of the efficiency of Fe-doped TiO_2 prepared by two doping methods and photocatalytic degradation of phenol in domestic water suspensions. Science and Technology of Advanced Materials. 2007, May; 8(4): 286 – 291.
45. Khan MA, Woo SI, Yang BO. Hydrothermally stabilized Fe (III) doped titania active under visible light for water splitting reaction. International Journal of Hydrogen Energy. 2008, October; 33(20): 5345 – 5351.
46. Alexandrescua R, Morjana I, Scarisoreanua M, Birjegaa R, Popovicia E, Soarea I, Gavrila-Florescua L, Voicua I, Sandua I, Dumitrachea F, Prodanb G, Vasilec E, Figgemeierd E. Structural investigations on TiO_2 and Fe-doped TiO_2 nanoparticles synthesized by laser pyrolysis. Thin solid Films. 2007, October; 515(24): 8438 – 8445.
47. Benck JD, Pinaud BA, Gorlin Y, Jaramillo TF. Substrate Selection for Fundamental Studies of Electrocatalysts and Photoelectrodes: Inert Potential Windows in Acidic, Neutral, and Basic Electrolyte. Plos One. 2014, October; 9 (10): 1-13.
48. Rajakumara G, Rahuman AA, Priyamvada B, Khannac VG, Kum DK, Sujine PJ. Eclipta prostrata leaf aqueous extract mediated synthesis of titanium dioxide nanoparticles. Materials Letters. 2012, February; 68: 115-117.
49. Gupta M, Sharma V, Shrivastava J, Solanki A, Singh A P, Satsangi VR, .Shrivastav, R. Preparation and characterization of nanostructured ZnO thin films for photoelectrochemical splitting of water. Bulletin of Materials Science. 2009, February; 32 (1): 23-30.
50. Lezner M, Grabowska E, Zaleska, A. Preparation and photocatalytic activity of iron-modified titanium dioxide photocatalyst. Physicochemical Problems of Mineral Processing. 2011, December; 48 (1): 193-200.
51. Bittmann B, Haupert F, Schlarb AK. Preparation of TiO_2/epoxy nanocomposites by ultrasonic dispersion and their structure property relationship. Ultrasonics Sonochemistry. 2011, January; 18(1):120 – 126.
52. Dai G, Zhao L, Wang S, Hu J, Dong B, Lu H, Li J. Double-layer composite film based on sponge-like TiO2 and P25 as photoelectrode for enhanced efficiency in dye-sensitized solar cells. Journal of Alloys and Compounds. 2012, October; 593: pp.264-270.
53. Keis K, Magnusson E, Lindstrom H, Lindquist S E, & Hagfeldt A. 5% efficient photoelectrochemical solar cell based on nanostructured ZnO electrodes. Solar Energy Materials and Solar Cells. 2002, May; 7(1): 51-58.
54. Lindstrom H, Magnusson E, Holmberg A, Sodergren S, Lindquist SE, Hagfeldt, A. A new method for manufacturing nanostructured electrodes on glass substrates. Solar Energy Materials & Solar Cells. 2002, May; 73(1): 91-101.
55. Acevedo-Peña P, González I, Vázquez G, Manríquez J. Generación de estados superficiales durante la formación electroforética catódica de películas de TiO2 sobre ito. Química Nova. 2011; 34(3).
56. Chauhan D, Satsangi VR, Dass S, Shrivastav R. Preparation and characterization of nanostructured CuO thin films for photoelectrochemical splitting of water. Bulletin of Materials Science. 2007; 9(7): 709 – 716.
57. Kilner JA, Skinner SJ, Irvine SJC, Ewards PP. Functional materials for sustainable energy applications. Cambridge – Published by Woodhead Published Limited. 2012. Chapter 3, Rapid, low – temperature processing of dye-sensitized solar cells; 42 – 66.
58. Hodes G. Photoelectrochemical Cell Measurements: Getting the Basics Right. The Journal of Physical Chemistry Letters. 2012; 3(9): 1208 – 1213.
59. Iaiche S, Djellou A. ZnO/$ZnAl_2O4$ Nanocomposite Films Studied by X-Ray Diffraction, FTIR, and X-Ray Photoelectron Spectroscopy. Journal of Spectroscopy. 2015; volume 2015. http://dx.doi.org/10.1155/2015/836859

60. Swanson HE, McMurdie H F, Morris M C, Evans E H. Standard X-ray Diffraction Powder Patterns. NBS Monograph 25 – Section 7. U.S. Department of Commerce-National Bureau of Standars. 1969
61. Gupta SM, Tripathi M. A review of TiO_2 nanoparticles. Physical Chemistry. 2010, June; 56 (16): 1639-1657. doi: 10.1007/s11434-011-4476-1
62. Hu Y, Tsai HL, Huang CL. Phase transformation of precipitated TiO_2 nanoparticles. Materials Science and Engineering: A. 2003, March; 344 (1-2); 209-214.
63. Nithya A, Rokesh K, Jothivenkatachalam K. Biosynthesis, characterization and application of titanium dioxide nanoparticles. Nano Vision. 2013, October; 3 (3): 169-174
64. Nwanya AC, Ugwoke PE, Ejikme PM, Oparaku Ou, Ezema FI. Jathropha Curcas and Citrus Aurantium leaves dye extract for use in dye sensitized solar cell with TiO2 Films. International Journal of Electrochemical Science. 2012; 7: 11219 – 11235.
65. Momeni MM, Ghayeb Y. Fabrication, characterization and photoelectrochemical behavior of Fe–TiO2 nanotubes composite photoanodes for solar water splitting. Journal of Electroanalytical Chemistry. 2015, August; 751: 43-48.
66. Lee T, Ryu H, Lee W. Photoelectrochemical properties of iron (III) – doped TiO2 nanorods. Ceramics International. 2015, July; 41(6): 7582 – 7589.
67. Wang CT, Siao HL, Chiu YC. Iron-doped titania thin films with enhanced photovoltaic efficiency: Effects of iron concentration and rectifying layer. Surface and Coatings Technology. 2013, October; 232: 658 – 665.
68. Ako RT, Ekanayake P, Young DJ, Hobley J, Chellappan V, Tan AL, Gorelik S, Subramanian GS, Lim CM. Evaluation of surface energy state distribution and bulk defect concentration in DSSC photoanodes based on Sn, Fe, and Cu doped TiO2. 2015, October; 351: 950 – 961.
69. Choudhury B, Dey M, Choudhury A. Defect generation, d-d transition, and band gap reduction in Cu-doped TiO2. International Nano Letters. 2013, December; 3(1).
70. Naceur JB, Mechiakh R, Bousbih F, Chtourou R. Influences of the iron ion (Fe3+)-doping on structural and optical properties of nanocrystalline TiO2 thin films prepared by sol–gel spin coating. Applied Surface Science. 2011, October; 257(24): 10699 – 10703.
71. Choi J, Park H, Hoffmann MR. Effects of Single Metal-Ion Doping on the Visible-Light Photoreactivity of TiO2. The Journal of Physical Chemistry. 2010; 114(2): 783 – 792.
72. Kim DH, Hong HS, Kim SJ, Song JS, Lee KS. Photocatalytic behaviors and structural characterization of nanocrystalline Fe-doped TiO2 synthesized by mechanical alloying. Journal of Alloys and Compounds. 2004, July; 375 (1-2): 259 – 264.
73. Liu, Y, Xu C, Feng, Z. Characteristics and anticorrosion performance of Fe-doped TiO2 films by liquid phase deposition method. Applied Surface Science. 2014, July; 314: 392-399.
74. Zhu J, Chen F, Zhang J, Chen H, Anpo M. Fe3+-TiO2 photocatalysts prepared by combining sol–gel method with hydrothermal treatment and their characterization. Journal of Photochemistry and Photobiology A: Chemistry. 2006, May; 180(1-2): 196-204.
75. Kravets VG, Grigorenko A. New class of photocatalytic materials and a novel principle for efficient water splitting under infrared and visible light: MgB2 as unexpected example. Optics Express. 2015; 23(24): A1651 – A1663.

*****